Exploring micropollutant biotransformation in three freshwater phytoplankton species

Michael A. Stravs[†‡], Francesco Pomati[†§], Juliane Hollender[†‡*]

[†]Eawag Swiss Federal Institute of Aquatic Science and Technology, Überlandstrasse 133, 8600 Dübendorf, Switzerland

[‡]Institute of Biogeochemistry and Pollutant Dynamics, Universitätstrasse 16, ETH Zürich, 8092 Zürich, Switzerland

[§]Institute of Integrative Biology, ETH Zürich, Universitätstrasse 16, 8092 Zürich, Switzerland

* Corresponding Author

Überlandstrasse 133, 8600 Dübendorf, Switzerland

phone: +41 58 765 5493; fax: +41 58 765 5893; e-mail: juliane.hollender@eawag.ch

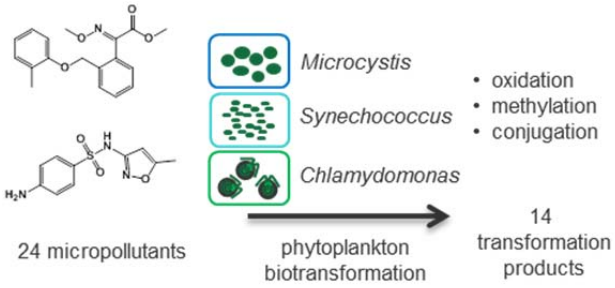

Abstract

Phytoplankton constitute an important component of surface water ecosystems; however little is known about their contribution to biotransformation of organic micropollutants. To elucidate biotransformation processes, batch experiments with two cyanobacterial species (*Microcystis aeruginosa*, *Synechococcus sp.*) and one green algal species (*Chlamydomonas reinhardtii*) were conducted. Twenty-four micropollutants were studied, including 15 fungicides and 9 pharmaceuticals. Online solid phase extraction (SPE) coupled to liquid chromatography (LC) – high resolution tandem mass spectrometry (HRMS/MS) was used together with suspect and nontarget screening to identify transformation products (TPs). 14 TPs were identified for 9 micropollutants, formed by cytochrome P450-mediated oxidation, conjugation and methylation reactions. The observed transformation pathways included reactions likely mediated by promiscuous enzyme reactions, such as glutamate conjugation to mefenamic acid and pterin conjugation of sulfamethoxazole. For 15 compounds, including all azole fungicides tested, no TPs were identified. Environmentally relevant concentrations of chemical stressors had no influence on the transformation types and rates.

This document is the accepted manuscript version of the following article:
Stravs, M. A., Pomati, F., & Hollender, J. (2017). Exploring micropollutant biotransformation in three freshwater phytoplankton species. *Environmental Sciences: Processes and Impacts*. http://doi.org/10.1039/C7EM00100B

Environmental impact

The persistence, fate and transformation of organic micropollutants in freshwater is frequently studied. However, a potential contribution of phototrophic organisms to micropollutant fate is often disregarded. Phytoplankton is a crucial component in freshwater ecosystems, yet little is known about its role in the fate of organic micropollutants, and formation of potentially unknown transformation products. The present study examines the biotransformation of a set of both wastewater-borne and agricultural micropollutants in three freshwater phytoplankton species, revealing biotransformation by common mechanisms and by promiscuous enzyme reactions. Understanding of biotransformation pathways in phytoplankton adds to the general picture of environmental fate processes, and has potential additional relevance for processes in algae-containing water treatment systems.

Introduction

Natural water bodies receive inputs of polar organic micropollutants from diffuse and point sources such as agricultural run-off and wastewater treatment plant effluents. The persistence of those micropollutants in the environment varies widely depending on biotic and abiotic processes such as photodegradation, microbial degradation, sorption, and potentially also bioaccumulation and biotransformation in different organisms.

For pesticides in agricultural use, fate studies concerning persistence, degradation, sorption, and other processes in water and sediment, as well as toxicity studies in different freshwater organisms (phytoplankton, invertebrates, fish) are mandatory for registration [1]. Similar tests are also mandated for pharmaceuticals [2]; however the corresponding data is usually confidential, and only in select cases is their fate known.

Specifically, aerobic and anaerobic transformation in water bodies is examined in Organisation for Economic Co-operation and Development (OECD) tests 308 and 309 [3,4]. Such tests are typically intended to examine biotransformation by heterotrophic microorganisms. In contrast, very little is known about bioaccumulation, biotransformation, or biodegradation in other aquatic organisms. Thomas and Hand [5] investigated the degradation of pesticides under conditions close to the OECD 308 guidelines, in the presence or absence of phytoplankton or macrophytes. They demonstrated that the presence of phototrophic organisms had significant effect on the degradation of certain pesticides. A closer investigation of the degradation of the fungicide fludioxonil showed metabolic activity of different strains of cyanobacteria, green algae and diatoms [6]. Studies on wastewater treatment in e.g. algal ponds and bioreactors also suggest that some micropollutants can be degraded by algae to different extents [7–10]. As phototrophs, phytoplankton do not rely on organic chemicals as carbon sources, however the presence of biotransformation in algae is potentially a detoxification mechanism, as suggested for dichlorophenol degradation [11], or a consequence of enzyme promiscuity or reactivity with compounds similar to their natural substrates (as suggested e.g. for *Arabidopsis* [12,13]).

This highlights the need to study the role of algae in biotransformation, as knowledge about biotransformation processes in phytoplankton is limited. Enzymes active in biotransformation are present in cyanobacteria and other microalgae. Cytochrome P450 enzymes are found in all domains of life [14]. They are widespread in green algae and cyanobacteria [15,16], and some are known to participate in biological functions, but many remain uncharacterized [15]. The activity of phytoplankton enzymes in biotransformation has been demonstrated; examples include cytochrome P450 (CYP450) monooxygenase, O- and N-glucosyltransferase and glutathione S-transferase activity on a number of substrates in marine macroalgae [17], or CYP450-dependent dealkylation of several ethers in *Chlorella* strains [18]. On the other hand, no studies to date include or imply the activity of promiscuous enzymes.

Biotransformation in phytoplankton has only been investigated for few compounds so far. For estrogens, glucose conjugation as well as hydroxylation and other oxidation/reduction reactions and hydrolysis

have been reported [19–21] but even unusual reactions such as bio-bromination [22] have been observed. In a study with different monoterpenes, various redox reactions were found [23]. Oxidation was also found to be important for the organophosphorus pesticide fenamiphos [24], whereas sulfate and glucose conjugation as well as O-methylation products were observed in the case of tetrabromobisphenol A [25]. O-methylation of the antimicrobial triclosan was also observed [26].

However, so far, no study has attempted to get a more comprehensive picture of the biotransformation potential of algae and cyanobacteria. Therefore, our goal was to investigate biotransformation processes in phytoplankton more closely, to elucidate important types of biotransformation reactions and determine relevant structural moieties susceptible to those reactions. To this end, we performed batch experiments to identify transformation products for 24 micropollutants (9 pharmaceuticals and 15 fungicides) with various functional groups. Within the fungicides, two groups of structurally related compounds (5 strobilurin fungicides and 9 azole fungicides) were selected to investigate commonalities within compound classes. The strobilurin fungicides are synthetic analogs of fungicidal natural products with a β-methoxyacrylate group or analog, acting on the respiratory chain, whereas azole fungicides are synthetic chemicals with an imidazole or triazole ring, which inhibit CYP450 enzymes in fungi[27]. Strobilurins are used only in agriculture, whereas azole fungicides have both agricultural and medicinal uses. We focused on the biotransformation behavior of two phytoplankton functional groups, the green algae (Chlorophyta) and the Cyanobacteria, which were also the main focus of Thomas and Hand's studies [6]. As a green alga, *Chlamydomonas reinhardtii* was studied, which is an important freshwater and soil alga and a well-studied model organism. For cyanobacteria, two related but physiologically different species were chosen: *Microcystis aeruginosa* and *Synechococcus sp.* are common freshwater phytoplankton species. *Microcystis aeruginosa* is a medium-sized (~5 µm cell size) cyanobacterium, forms colonies in natural conditions, and frequently causes harmful algal blooms, while *Synechococcus* is the most abundant component of the picoplankton (<1 µm) in aquatic ecosystems. Degradation of the substance mixture over time and the formation of transformation products (TPs) was characterized with liquid chromatography – high-resolution tandem mass spectrometry (LC-HRMS/MS). To investigate the induction of biotransformation as a general stress response mechanism, the influence of low-level environmental stressors on the transformation was simulated by three algicides.

Materials and Methods

Chemicals. All organic micropollutants were obtained in analytical grade (typically 98%+) from Dr. Ehrenstorfer (now LGC Standards, Wesel, Germany), Sigma-Aldrich (St. Louis, MO, USA), Fluka (now Sigma-Aldrich), TRC Canada (Toronto, Canada), Novartis (Basel, Switzerland) or HPC Standards (Cunnersdorf, Germany). A detailed list is attached in Table S1. Two mixtures of chemicals were used in experiments (Mix 1, all compounds, and Mix 2, no azoles): atenolol (ATE), bezafibrate (BEZ), carbendazim (CBDZ), mefenamic acid (MEF), metoprolol (MPL), ranitidine (RAN), tramadol (TRA), venlafaxine (VFX), verapamil (VPL), azoxystrobin (AZY), fluoxastrobin (FXS), kresoxim-methyl (KME), pyraclostrobin (PYR) and trifloxystrobin (TFL) were contained in both Mix 1 and Mix 2. Cyproconazole (CYP), difenoconazole (DIF), epoxiconazole (EPO), fluconazole (FLU), ketoconazole (KET), metconazole (MET), penconazole (PEN), propiconazole (PRO), tebuconazole (TEB) and sulfamethoxazole (SMZ) were only contained in Mix 1. Before analysis, samples were fortified with an in-house isotope-labeled internal standard (IS) mixture; the standards used for quantification are listed in Table S2.

Cultures. *Microcystis aeruginosa*, strain PCC7806 (*Mcy*), *Synechococcus sp.*, natural isolate from a Swiss lake (*Syn*), and *Chlamydomonas reinhardtii*, strain CC125 (*Chl*), were obtained from subsampling of in-house cultures. Cultures were kept at room temperature in 100 mL Erlenmeyer flasks. *Mcy* and *Syn* were grown in WC (Woods Hole Combo, see SI) medium, whereas *Chl* was grown in WC+A+M medium (with ammonia and MOPS, see SI). Cultures were kept under ambient light and room temperature for

maintenance. Subculturing was performed under sterile conditions in a clean bench close to a Bunsen burner flame.

Single species experiments. Biotransformation experiments were conducted in an incubation shaker (Multitron II, Infors HT, Bottmingen, Switzerland) at 20°C, 90 rpm at approximately 100 µEinstein of light intensity from fluorescent tubes. To inhibit possible phototransformation, the fluorescent tubes were equipped with UV protection tubes (METOLIGHT ASR-UV-400-60-T8, Asmetec, Germany) and the shaker window was covered with UV protection foil (METOLIGHT SFC-10, Asmetec, Germany). One week before the start of the experiment, maintenance cultures of *Mcy*, *Syn* and *Chl* were transferred into fresh WC medium (*Mcy*, *Syn*) or WC+A+M medium (*Chl*) and incubated under experimental conditions. At the start of the experiment, for each species 6 subcultures of 50 mL were prepared in sterile 100 mL Erlenmeyer flasks. To 3 flasks, Mix 1 (see above and Table S1; 1 mg/L per compound in EtOH) was added to a final concentration of 10 µg/L per substance. To one flask, Mix 2 (without azoles, 1 mg/L in EtOH) was added to a final concentration of 10 µg/L per substance. To two control flasks, only solvent (500 µL EtOH) was added. In addition, two flasks were prepared with 50 mL WC or WC+A+M medium, and chemical mixture 1 was added to a final concentration of 10 µg/L per substance. All samples were then incubated as described above.

Immediately after addition of the chemical mixture (t0), and after 1 (t1) and 4 days (t2), samples were taken for chemical analysis and cell density measurement. After 12 days (t3), an additional sample of only the medium was taken, as algal cultures were in senescent state. For chemical analysis, 10 mL per culture were sampled into a glass centrifuge tube pre-washed with MeOH and centrifuged 2 min at 4000 rpm (*Mcy*, *Chl*) or 20 min at 4000 rpm (*Syn*) (PerfectSpin 24 Plus, Peqlab, Germany). 1 mL of supernatant was transferred into an HPLC vial and stored at -20°C. The remaining supernatant was discarded. As a washing step to remove chemicals from residual medium or weakly adsorbed to cells, the pellet was resuspended in 10 mL WC medium in a fresh tube and centrifuged again for 2 min at 4000 rpm (*Mcy*, *Chl*) or 20 min at 4000 rpm (*Syn*). The supernatant was discarded. The pellet was resuspended in 1 mL nanopure H_2O and frozen in liquid N_2, then stored at -20°C until analysis. For cell density measurement, 200 µL per culture were sampled into a 96-well plate, and optical density at 680 nm and 750 nm was measured (SpectraMax 190, Molecular Devices, Sunnyvale CA). The biomass per sample was determined from a calibration curve to dry weight, which was previously generated for the three species.

Sample preparation. Concentrations of all chemicals in the growth medium was determined from the supernatant, and internal concentrations were determined from the pellet. For measurement of medium concentration, 100 µL supernatant was diluted to 20 mL with nanopure water and fortified with IS mixture (total final absolute amount 1 ng IS per substance and sample). For measurement of internal concentrations, cells in the pellet were lysed by three cycles of freezing in liquid N_2 and thawing at 37°C in an ultrasonic bath, and subsequently frozen in liquid N_2 and freeze-dried. The lyophilized samples were redissolved in 1 mL MeOH and 1 mL nanopure H_2O, then briefly sonicated in an ultrasonic bath at 37°C. The samples were centrifuged for 1 min at 4000 rpm. 750 µL supernatant was diluted with nanopure H_2O to 20 mL and IS was added (total final absolute amount 1 ng IS per substance and sample).

Chemical Analysis. Samples were analyzed by online solid phase extraction coupled to high performance liquid chromatography – high resolution tandem mass spectrometry (online SPE – LC – HRMS/MS) as described previously [28]. To 20 mL sample, 80 µL 0.5M citric acid buffer (pH 7) were added. The entire sample was loaded into a sample loop and enriched on a mixed-bed multilayer online SPE cartridge (see SI, loading solvent: 2 mM ammonium acetate in H_2O, pH 7). Separation was performed on an Atlantis T3 column (3 mm × 150 mm; Waters Milford, USA), For chromatography, a gradient was formed by mixing water (A, H_2O / 0.1% formic acid (FA)) and organic solvent (B, MeOH / 0.1% FA) delivered by two separate pumps (total flow rate: 300 µL/min, gradient: 13.3% B (0-5 min), 13.3 to 95% B (5-20 min), 95% B (20-29 min), 95 to 13.3% B (29-29.5 min), 13.3% B (29.5-35 min;

reconditioning)). For 7 min, solvent B ran over the SPE cartridge (elution of enriched analytes) before mixing with A (dilution before analytical column). During cartridge elution, the sample loop was washed with acetonitrile (1 min, 4 mL/min). During chromatography, the cartridge was washed with acetonitrile (5.1 min, 0.4 mL/min) and reconditioned with loading solvent (5.5 min, 0.4 mL/min), and subsequently the next sample was enriched on the cartridge (16 min, 1.27 mL/min).

Detection was performed using a quadrupole-Orbitrap mass spectrometer (Q-Exactive Plus, Thermo Scientific, Bremen) with a heated electrospray (H-ESI) source. For quantification measurements, data was acquired in polarity switching mode with data-dependent acquisition with an MS^2 inclusion list. For the inclusion list, masses of the parent compounds and masses of potential metabolites calculated using mass differences (hydroxylation, demethylation, didemethylation, dehydration) in positive and negative modes were selected. For acquisition of MS^2 spectra for compound identification, selected samples were reanalyzed in targeted MS^2 mode. Detailed parameters are listed in the SI.

Quantification of analytes using the internal standard method was performed with TraceFinder EFS (version 3.2.368.22, Thermo Scientific, Bremen). Table S2 lists internal standards used for quantification for each analyte. A mass tolerance of 5 ppm was allowed. Analyte peaks were automatically integrated by the ICIS algorithm and reviewed by hand. Where available, the internal standard used for quantification was the isotope-labeled analyte. Otherwise, an internal standard close in retention time and with a similar structure was used. All spiked parent compounds as well as known TPs available in the lab as authentic standards (see Table S2) were quantified. In addition, newly identified TPs were added retrospectively to the analysis and quantified as area relative to the parent compound, which disregards differences in ionization and is therefore only an indicative measure. Calibration curves were weighted 1/x over the concentration range. For lysate samples, calculated biomass was used to convert substance amount to dry weight concentrations.

Screening and structure elucidation of transformation products (TPs)

Suspect and nontarget screening of TPs were conducted using the open-source workflow RMassScreening (https://www.github.com/meowcat/RMassScreening). It integrates feature detection using the enviPick R package (https://www.github.com/blosloos/enviPick), and cross-sample feature alignment (profile building) using the enviMass R package (https://www.github.com/blosloos/enviMass). For grouping of isotopes, adducts and in-source fragments (componentization), a customized version of the R package RAMClustR [29] was used (https://www.github.com/meowcat/RAMClust). A list of potential TPs was generated from the parent compounds, using lists of possible modifications that were applied for one or two generations using RMassScreening (see Table S3 for lists). Suspect hits were found based on exact mass matches from screening the list on all found profiles.

Time series filtering, implemented in RMassScreening, was applied to the features such that 1) only features not present in the micropollutant-free controls were retained, 2) only features absent or with small intensity at t0 were retained, and 3) only features present in chemical treatment groups, but absent in medium control were retained. The list was ordered by decreasing intensity in the chemical treatment. Typically, filters were set to include features 3x over intensity at t0 and in abiotic and chemical controls. The resulting list was evaluated visually to find products with a trend consistent with TPs. These criteria were applied either to suspect hits (for suspect screening), or to all profiles (for nontarget screening).

For putative TPs, MS^2 spectra were initially extracted (if available) from the original measurements, and later acquired with targeted MS^2 at multiple collision energies for detailed MS^2 analysis. Spectra were extracted using RMassBank [30], and converted to MassBank [31] format version 2 (http://www.massbank.jp). Fragment mass spectra were interpreted manually with help of known fragment mass spectra of parent compounds and in silico methods. MS^2 elucidation was aided by the package MassInSpectoR (https://github.com/meowcat/MassInSpectoR). This toolkit interfaces to GenForm [32] (https://sourceforge.net/projects/genform) for parent formula assignment based on MS and MS^2 spectra, and fragment/loss annotation, CFM-ID [33,34] for prediction of MS^2 spectra of unknown

compounds, and RMassBank [30] and in-house code for spectra comparison and shifting. The mass spectral databases MassBank [31] (http://www.massbank.jp), MoNA (http://mona.fiehnlab.ucdavis.edu), and METLIN [35] (https://metlin.scripps.edu/index.php) were used for similarity searches. Identification confidence was stated according to the guidelines by Schymanski *et al*. [36].

Results and Discussion

Overview

A mixture of 24 compounds was used for incubation experiments (Mix 1, see in detail Table S1.) The mixture covers a wide range of physicochemical properties, with molecular weight from 191 to 531 Da, and log octanol-water partitioning coefficient (log Kow) values from 0.16 to 5.12. The compounds span a range of functional groups, including secondary and tertiary amines, carboxylic acids, esters and amides, sulfonamides, alcohols, ethers, cyanides, triazoles, epoxides, and compounds with and without halogens. In preliminary tests, it was verified, both as single compounds and in mixtures, that the compounds used do not significantly inhibit growth in single species experiments at concentrations of 10 and 100 µg/L, as reflected in the growth curves for single species and mixture experiments (Figure S1). Fourteen of the 24 compounds (Mix 2, excluding azole fungicides and sulfamethoxazole) were tested separately to evaluate a potential inhibitory effect on biotransformation (see below). Strongly algicidal compounds (triclosan, atrazine, irgarol) had been excluded from the mixture after initial tests; these compounds were used as chemical stressors (see below). The mixtures (Mix 1 or Mix 2) were applied to batch cultures of the single species *Mcy*, *Syn* and *Chl* or a *Mcy*+*Syn* mixture (see SI) at a concentration of 10 µg/L per compound to study bioaccumulation and biotransformation of the compounds. Cultures grew from 0.07 to 0.25 mg/L dry weight (DW) equivalent (*Mcy*), 0.06 to 0.21 mg/L DW (*Syn*) and 0.01 to 0.07 mg/L DW (*Chl*), respectively, over the course of 4 days in single species experiments, and from 0.04 to 0.15 mg/L DW in *Mcy*+*Syn* mixture experiments (Figure S1). (Note: *Chl* was not used in combination experiments, since the strain used needs an adapted growth medium.)

Internal concentrations: fast equilibration and log K_{ow}-dependent accumulation

For all compounds and species, bioconcentration factors (BCFs) were calculated as the mean of all values during apparent equilibrium. Some compounds (CBDZ, FLU, TRA, VFX) did not accumulate in the cells at all (*i.e.*, internal concentrations < LOD), whereas for DIF, PYR and TFL the highest observed BCF values were close to 1000 (see Table S5). For all compounds, the observed log BCF factors showed a weak correlation with log K_{ow}. Within the two studied compound classes alone, the correlation was stronger (R^2 >0.7 in all cases, see Table S6 and Figure S2), which is likely because physicochemical properties within the classes are more homogenous, and all compounds are uncharged under experimental conditions. Differences between the studied species were insufficient to warrant any conclusions. Fast equilibration was generally observed: for many compounds, the apparent BCF reached a stable value already at the first sampling point (t0, effectively ca. 30 min). Notably, fast equilibration could lead to BCF underestimation, since compounds could be lost to the medium in the wash step (see Materials and Methods). A summary of the compound mass balances in the three species after four days (Table S4) shows that for many compounds the largest fraction remained in the medium.

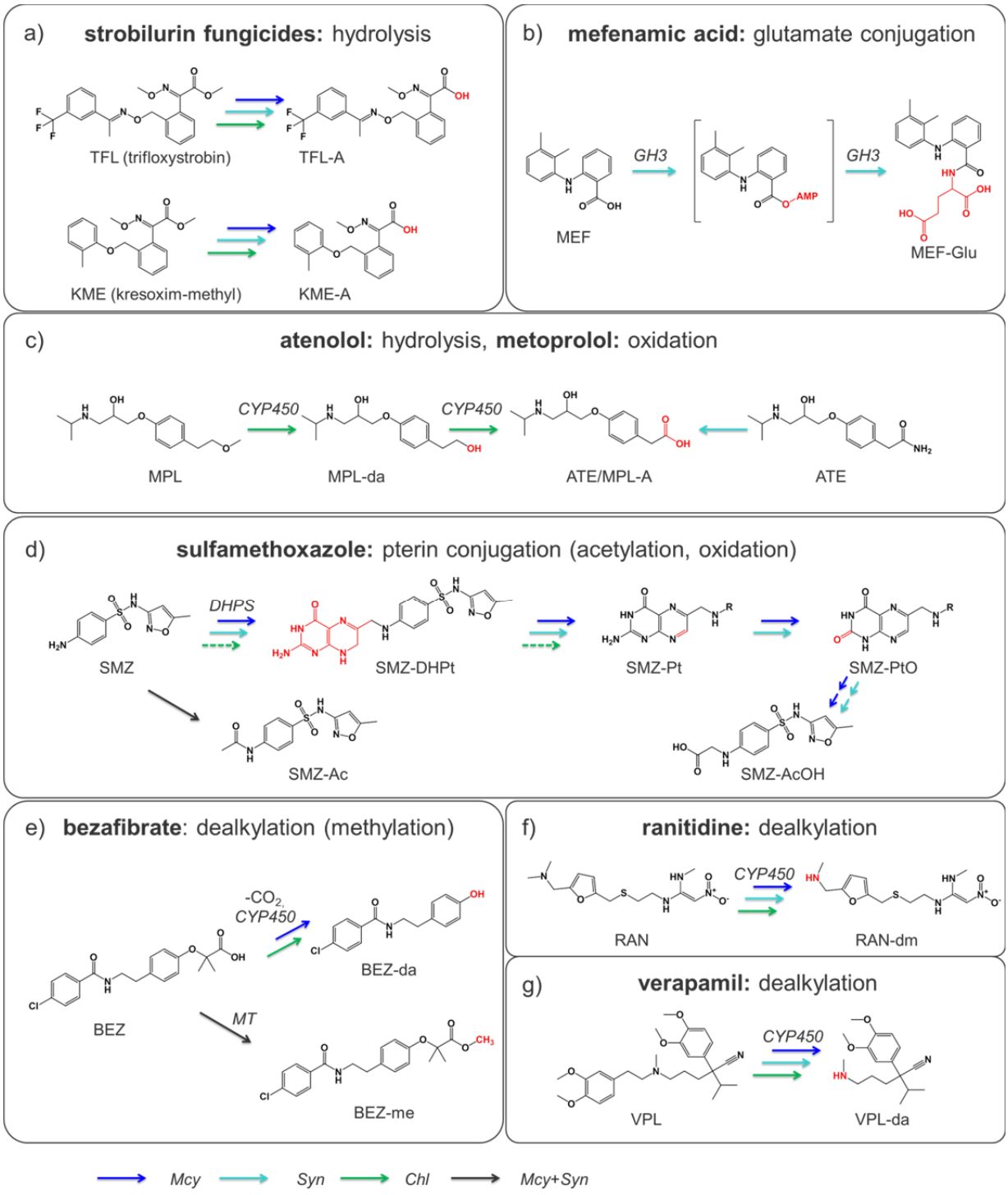

Figure 1: Observed biotransformation pathways and products for a) strobilurin fungicides, b) mefenamic acid, c) atenolol and metoprolol, d) sulfamethoxazole, e) bezafibrate, f) ranitidine and g) verapamil. Italic: putative enzyme responsible for reaction. Arrows: species exhibiting the reaction. Blue: *Mcy*, light blue: *Syn*, green, *Chl*, black: only observed in mixture experiments. GH3: Gretchen Hagen 3. DHPS: dihydropteroate synthase. CYP450: cytochrome P450. MT: methyltransferase. Note that transformed functional groups are in red. Dashed arrows: minimal amounts of SMZ-Pt detected in *Chl*.

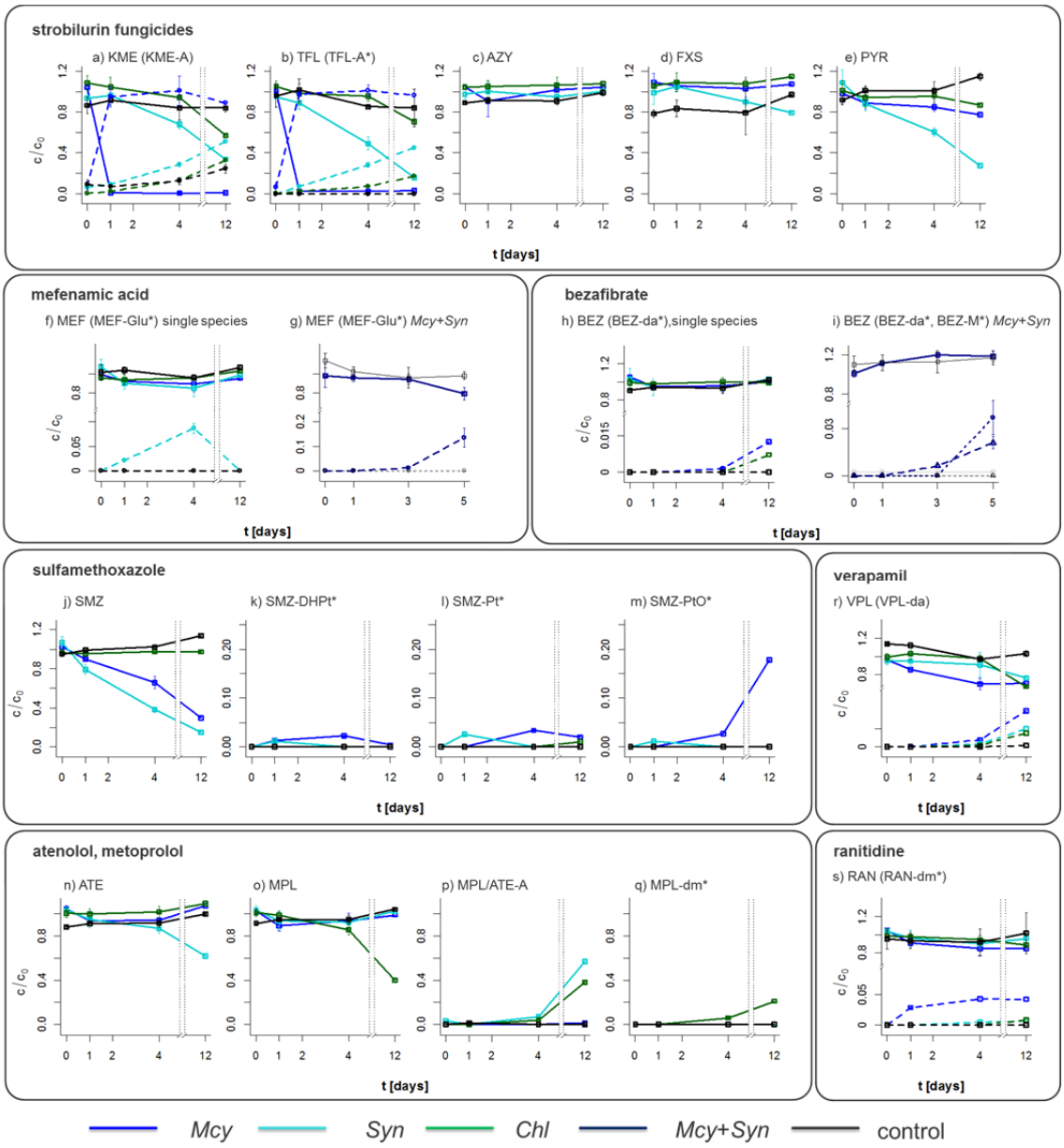

Figure 2: Biotransformation of micropollutants, time profiles. c/c_0 values are concentrations, or transformation product amounts semiquantified via peak area (marked *), relative to average initial parent concentration. a)-e) Strobilurin fungicides in single-species experiments. Bold lines: concentration in medium. Solid lines: a) KME, b) TFL, c) AZY, d) FXS, e) PYR. Dashed lines: a) KME-A, b) TFL-A. f)-g) MEF biotransformation in single-species (f) and *Mcy+Syn* mixture (g) experiments. Solid lines: MEF, dashed lines: MEF-Glu. h)-i): BEZ biotransformation in single-species (h) and *Mcy+Syn* mixture (i) experiments. Solid line: BEZ, dashed lines: BEZ-dm, dotted line: BEZ-M. j)-m): SMZ biotransformation in single-species experiments. j) SMZ, k) SMZ-DHPt, l) SMZ-Pt, m) SMZ-PtO. n)-q): MPL and ATE biotransformation in single-species experiments. n) ATE, o) MPL, p) ATE/MPL-A, q) MPL-dm. r) Biotransformation of VPL in single-species experiments. Solid line: VPL, dashed line: VPL-da. s) Biotransformation of RAN in single-species experiments. Solid line: RAN, dashed line: RAN-dm. Blue: *Mcy*, turquoise: *Syn*, green: *Chl*. Black: medium control. g), i): Dark blue: *Mcy+Syn* mixture.

Fate of strobilurin fungicides

Of the five strobilurin fungicides tested (AZY, FXS, KME, PYR; TFL), fast disappearance was observed for KME and TFL in *Mcy*, while slower degradation was seen in *Syn* and *Chl* (Figure 2a, b). AZY was essentially stable in the medium (Figure 2c). PYR and FXS, which are the most apolar of the five, showed disappearance from the medium over time in *Syn*, but not in *Mcy* or *Chl*. For both, accumulation in cells could be observed, which could, however, not completely account for the losses in medium (Figure 2d-e).

Through suspect screening and MS^2 interpretation, the ester hydrolysis products (kresoxim-methyl acid (KME-A, $[M+H]^+$ 300.1234, RT 23.4 min) and trifloxystrobin acid (TFL-A, $[M+H]^+$ 395.1213, RT 23.9 min) could be identified as TPs (Figure 1a). The identity of KME-A could be confirmed by authentic standard. TFL-A, which had been observed in a preliminary study [37], was later also confirmed with an authentic standard. As shown in Figure 2a, the formed KME-A accounts for nearly 100% of KME dissipated; TFL-A (only quantified using relative area since at the time the standard was not available) is also the near-quantitative TP of TFL (Figure 2b). For PYR and AZY, the corresponding hydrolysis product was not observed, even though for AZY it is a known microbial metabolite [38]. FXS is not amenable to hydrolysis because of its lack of an ester function.

Small amounts (<10%) of KME-A and TFL-A were also formed in the medium control (see Figure 2a-b). Since both can hydrolyze abiotically at basic pH with half-lives of 7 h and 27.1 h at pH 9 [39], their fast formation in biological samples could in principle be due to pH shifts in the medium during growth. Therefore, combination (*Mcy*+*Syn*) experiments were performed with medium at pH 7.2 or 7.5 and medium pH was followed during the experiment (see Figure S3). As a control, autoclaved phytoplankton mixture was used to include abiotic reactions mediated by dead cyanobacterial cells. While in this experiment, disappearance of KME and TFL was less rapid and did not go to completion, it could be observed that 1) the pH was stable for 3 days during the experiment, and 2) a higher pH did not lead to faster hydrolysis, in fact at pH 7.2 hydrolysis proceeded faster. Biotic transformation at pH 7.2 was 8-fold (TFL-A) or 6-fold (KME-A) higher than abiotic TP formation. Therefore, it appears that the observed hydrolysis is linked to active cyanobacterial metabolism. Two possible alternatives remain to be investigated: 1) the hydrolysis is enzymatic or 2) it is driven by highly local pH changes that occur during photosynthesis, when CO_2 is depleted around cells.

With regards to the unexplained losses of PYR and FXS, no additional TPs could be identified. Since the substances are considerably hydrophobic, it is conceivable that the unexplained part of the mass balance indeed represents substance weakly adsorbed to the cells which is lost during the washing step.

Atenolol and metoprolol transformation

The TP atenolol/metoprolol acid (ATE/MPL-A, $[M+H]^+$: 268.1542, RT 13.6 min) was detected in single species experiments with both *Syn* and *Chl* species, and confirmed with an authentic standard. ATE/MPL-A is known to be formed from ATE by enzymatic hydrolysis [40], or from MPL by CYP450-mediated dealkylation [41,42] in human metabolism and microbial biotransformation. The disappearance of ATE in *Syn*, and of MPL in *Chl*, support the activity of the respective pathways in the two species (Figure 1c, Figure 2n,o). While the formation of ATE/MPL-A can fully explain the removal of ATE in *Syn*, the sum of ATE/MPL-A and MPL in *Chl* only account for ~80% of the original MPL quantity (Figure 2p). In addition to ATE/MPL-A, suspect screening revealed a second putative TP MPL-dm ($[M+H]^+$: 254.1750, RT: 13.1 min) consistent with a demethylation product of MPL (Figure 1c), which could be tentatively identified by MS^2 interpretation (see SI S3.10). This product, approximately quantified by area ratio (no authentic standard available), accounts for the remaining 20% of MPL removed (Figure 2q). Knowledge from human metabolism [43] suggest that MPL-dm is the precursor of MPL-A and would be degraded further to the latter.

Transformation of sulfamethoxazole

Five TPs of SMZ were identified (Figure 1d). A TP with $[M+H]^+$ 430.0930 (RT: 16.2 min) was initially thought to be a glucuronide conjugation product ($[M+H]^+$ 430.0915). However the MS^2 spectrum could not be reconciled with a glucuronide conjugation. A second TP with $[M+H]^+$ 429.1086 (RT 16.1 min) was initially matched as a second-generation TP by an amination reaction, and exhibited near-identical losses in the MS^2 spectrum. By MS^2 interpretation (see SI S3.4) and using information from previous studies [44], the latter could be tentatively identified as the TP pterin-sulfamethoxazole (SMZ-Pt). Sulfonamide drugs act as inhibitors of dihydropteroate synthase (DHPS) [45–47] which is expressed in microorganisms and plants, but not in higher eukaryotes [48]. DHPS catalyzes the formation of dihydropteroate from dihydropterin pyrophosphate and p-aminobenzoic acid, and sulfonamide antibiotics can act as an enzyme substrate and form a pterin conjugate [44,46]. The TP with $[M+H]^+$ 430 can then be explained as a product of SMZ-Pt (SMZ-PtO, see SI S3.5), where the primary amine has been transformed to a keto group. Through expanded screening, a third related product was observed, which is the dihydro form of SMZ-Pt (SMZ-DHPt, $[M+H]^+$ 431.1244, RT 15.9 min), whereas the dihydro form of SMZ-PtO was not found. In *Mcy* single culture experiments, SMZ-DHPt appears before SMZ-Pt and SMZ-PtO but disappears before the final timepoint (Figure 2j-m). This supports the formation pathway postulated by Richter et al. [44], which suggest SMZ-Pt as the stable form of SMZ-DHPt, and further the formation of SMZ-PtO from SMZ-Pt (rather than through a parallel pathway).

Additional TPs could be found at $[M+H]^+$ 312.0646 (RT 16.1 min) for single-species and *Mcy*+*Syn* combination experiments, and $[M+H]^+$ 296.0700 (RT 16.8 min) only in *Mcy*+*Syn* combination experiments (see Figure S4). The latter is the known metabolite N4-acetylsulfamethoxazole (SMZ-Ac), as confirmed by authentic standard. The former appeared to be N4-hydroxyacetyl-sulfamethoxazole, earlier observed by Majewsky et al. [49,50]; however comparison with an authentic standard (a gift of Dr. Marius Majewsky, Heidelberg, Germany, and Rafael Peschke, Karlsruhe, Germany) showed slight differences in retention time and markedly different MS^2 spectra in positive and negative mode. Based on MS^2 interpretation the compound appears to be sulfamethoxazole-N4-acetic acid (SMZ-AcOH, SI S3.6), possibly arising from a degradation of SMZ-Pt/SMZ-PtO. Both compounds reach only low concentrations (<3%), indicating that the products can be formed, but their relative importance is only minor to overall biotransformation.

CYP450 transformation products of pharmaceuticals

For BEZ, VPL and RAN, no significant dissipation was observed; however TPs were found in low concentrations (Figure 2h,i,r,s). Dealkylation products were observed that are consistent with CYP450 biotransformation (VPL-da, $[M+H]^+$: 291.2067 RT: 17.2 min, BEZ-da, $[M+H]^+$: 276.0787, RT: 21.39 min, RAN-dm, $[M+H]^+$: 301.1329, RT: 10.6 min; Figure 1e,f,g). VPL-da corresponds to the previously known VPL TP D617 [51] and was confirmed with authentic standard. Neither of the demethylation products (norverapamil by N-demethylation, or the O-demethylation products known as D702 and D703 [51]) was observed. BEZ-da was tentatively identified by MS^2 interpretation (see SI S3.7) and is hypothesized to arise from a decarboxylation followed by CYP450-mediated O-dealkylation. RAN-dm corresponds to the product of a mono-dealkylation on the dimethylamine of RAN (see SI S3.9), which is a known minor human RAN metabolite [52] but to our knowledge has not been observed in an environmental context. All three products were formed predominantly in *Mcy*, and in smaller quantities in *Chl* and *Syn*, except for BEZ-da, which was not formed in Syn. BEZ-da and RAN-dm could be observed in *Mcy*+*Syn* experiments; VPL-da was also present, but could not be quantified due to matrix interferences. These results suggest the activity of CYP450 enzymes in multiple biotransformation pathways in all three studied species. For further verification of the suggested pathways CYP450 inhibitors such as 1-aminobenzotriazole or piperonyl butoxide could be used in the future.

An additional methylation product was detected only in *Mcy*+*Syn* mixture experiments for BEZ (BEZ-M, $[M+H]^+$: 376.1310, RT: 23.3 min) with up to 5% relative area ratio (Figures 1e and 2i). The MS^2 spectrum

is consistent with a methyl ester formation, which is likely a regular methyltransferase-mediated reaction (see SI S3.8).

Glutamate conjugation of mefenamic acid

Suspect screening revealed a MEF TP at $[M+H]^+$ 371.1610 (MEF-Glu, RT: 23.28) consistent with a glutamic acid (Glu) conjugation product (Figure 1b). The product was observed in single species experiments with *Syn* and in *Mcy*+*Syn* mixture experiments (Figure 2f,g), reaching up to 12% area ratio relative to parent after 4 days. MS^2 interpretation supports the presence of a Glu conjugate (while not explicitly ruling out a possible isomer, a 2-methylaspartate conjugate, see SI S3.1). It is known from human metabolism that MEF can form activated ester derivatives, namely MEF-adenylate (AMP) and MEF-coenzyme A (CoA). Such activated esters are nonenzymatically reactive with biological nucleophiles including amino acids [53]. However we found no evidence for conjugation to any other amino acid. Specific conjugation to amino acids has been observed in plants, e.g. in the biotransformation of benzotriazole [12] and synthetic auxin herbicides such as 2,4-D [54]. Notably, enzymes of the GH3 family catalyze the conjugation of carboxylic acids to amino acids via an AMP intermediate, without the need for a CoA intermediate [55,56]. A search in the IMG/M database [57,58] (see SI) reveals a number of putative GH3 genes in cyanobacteria and specifically in *Synechococcus* species, but to our knowledge their biological functions have not yet been described. A number of GH3 enzymes are specific to plant hormones such as indole-3-acetic acid and jasmonic acid. However, other substrates are also known; in a reaction very similar to the observed one, the enzyme GH3.12 in *Arabidopsis thaliana* conjugates benzoic acids with glutamate specifically [59], which is thought to aid in the regulation of chorismate pathways. Glu or other amino acid conjugation products were not observed for other acids in the mixture such as BEZ or the hydrolysis products TFL-A, KME-A or MPL/ATE-A.

Transformation rate comparison, and persistent compounds

To place the observed transformations in context, we exemplarily compared transformation rates for ATE to known environmental degradation rates (see SI S2.5). Degradation rates in river water from available OECD 309 environmental fate data are between 0.004 d^{-1} and 0.025 d^{-1} [60]. Under exemplary eutrophic conditions and algal biovolumes (4 mm^3/L), we roughly estimate assuming biomass-normalized first-order transformation that the observed transformation would account for maximally 0.6% to 4%. This indicates that phytoplankton are not primary contributors to degradation for this example, in particular since phytoplankton represent a complex community and potentially only a fraction of all present organisms exhibit some degradation capability. On the other hand, the contribution could be more relevant in the case of monospecies blooms with particularly high biovolume [61].

For CBDZ, a product consistent with a methylation was observed, however, control experiments revealed that this likely originated from a transesterification with ethanol present in the mixture (see SI S2.3). For 13 out of the 24 tested compounds, no TPs and no degradation was observed. This notably includes all azole fungicides (CYP, DIF, EPO, FLU, MCZ, PEN, PRO, TEB) except for KET (see SI S2.4). Other compounds with no apparent biotransformation were TRA, VFX, and the three strobilurin fungicides already described above (AZY, FXS and PYR). Azole fungicides undergo various oxidative and conjugative transformations in mammals, plants and soil [62] but inhibit CYP450 enzymes in fungi and other organisms [27], including some algae [63], which could interfere with biotransformation. In microbial systems, VFX typically yields demethylation products [41] and N-oxides [64]. However, microbial systems are typically highly diverse, i.e. contain >1000 species [65], with a broad range of biotransformation capabilities.

Influence of chemical stressors

Two antagonistic potential factors that could influence biotransformation were examined. For one, other compounds present in the mixture could inhibit biotransformation, leading to an underestimation of the biotransformation potential. In particular, as azole fungicides are known CYP450 inhibitors, their

presence in the mixture could potentially inhibit biotransformation of other compounds [63,66]. Additionally, sulfamethoxazole is an antibiotic, and likely the most toxic compound in the mixture, with EC_{50} values reported for some phytoplankton organisms values in the sub-100 µg/L range [67]. On the other hand, toxic chemicals can induce biotransformation enzymes, as is known e.g. for atrazine and triclosan in rat liver [68,69]. It is possible that such chemical stressors, especially if being specifically toxic against green algae or cyanobacteria, could stimulate biotransformation of other compounds when present in environmentally relevant (but not acutely toxic) concentrations. Triclosan is an antimicrobial highly toxic against cyanobacteria and algae (EC_{50} for *Scenedesmus subsipcatus*: 0.7 µg/L, for *Anabaena flos-aquae* 0.97 µg/L) [70], while atrazine and irgarol are triazine herbicides, and toxic to algae and cyanobacteria as photosystem II inhibitors [71] (EC_{50} for *Synechococcus sp.* 45 µg/L [72] and 4.8 µg/L [73], respectively).

To test these hypotheses, incubation experiments with a *Mcy*+*Syn* mixture were performed. The culture was incubated with a chemical mixture of 24 (including azoles) or 14 (excluding azoles, see Table S1) compounds at 10 µg/L per compound. The experiments with both mixtures were performed in presence or absence of a chemical stressor at realistic environmental concentrations (0, 10 or 100 ng/L of atrazine, irgarol, or triclosan).

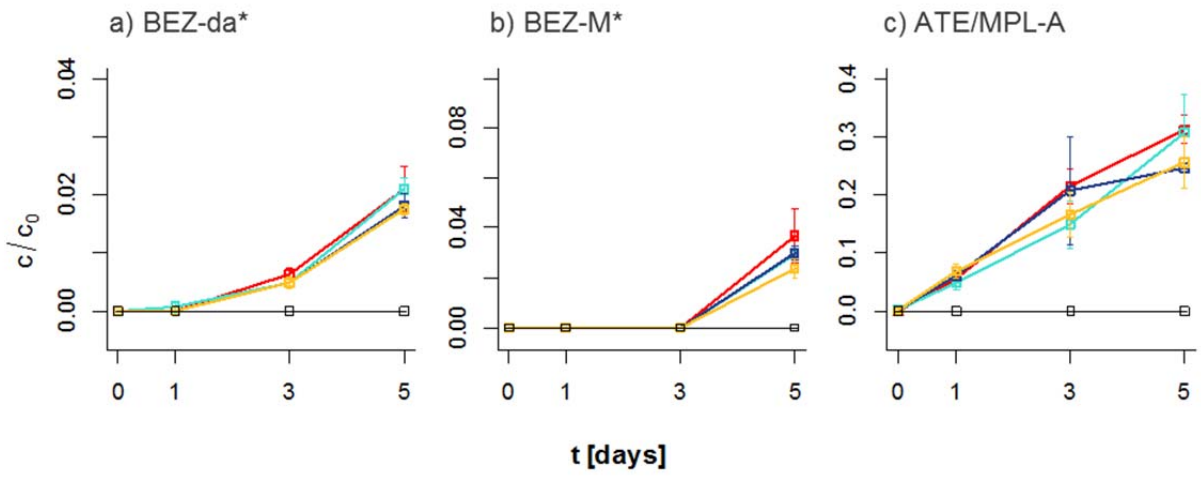

Figure 3. Formation of the TPs BEZ-da (a), BEZ-M (b) and ATE/MPL-A (c) under chemical stress. Blue: no atrazine / no azoles; red: azoles only, yellow: atrazine only, light blue: atrazine and azoles. c/c_0 values are concentrations, or transformation product amounts semiquantified via peak area (marked *), relative to average initial parent concentration.

Figure 3 shows the time profiles of bezafibrate dealkylation (a), bezafibrate methylation (b) and atenolol / metoprolol acid formation (c) with or without azoles and with or without 100 ng/L atrazine. If azoles inhibit biotransformation by CYP450 enzymes on a general scale, a faster formation of bezafibrate would be expected in their absence (while bezafibrate methylation and atenolol acid formation from atenolol can proceed without CYP450 contribution). Stimulation of biotransformation by atrazine would be apparent in faster formation rates of all three products. None of the studied experimental factors resulted in faster formation of observed TPs. Also, all previously stable compounds remained persistent, and no additional TPs were found by screening. The same results were observed for 10 ng/L atrazine and 10 or 100 ng/L irgarol or triclosan (Figure S5). The azole-free mixture was also tested in the original single species experiments without resulting in obvious changes. While it cannot be excluded that other conditions could potentially stimulate biotransformation (e.g. at higher concentrations less typically observed in the environment), the observed transformation potential of the tested species is seemingly neither limited by inhibition from azoles, nor enhanced by environmentally relevant concentrations of chemical stressors. Other environmental stressors, such as nutrient limitation and temperature, could potentially affect biotransformation and would be an interesting topic for follow-up studies.

Conclusion

This work provides insight into common and previously unknown transformation processes occurring in phytoplankton. In total, 14 TPs were identified for 9 parent compounds by various reactions. Of these, 3 involved hydrolysis, 5 involved CYP450 oxidation reactions of the parent compound, 4 were methylation or conjugation reactions and 3 involved modifications of a conjugate. Notably, multiple pathways likely result from enzymes reacting with non-natural substrates, such as MEF glutamate conjugation and SMZ pterin conjugation. Such reactions are not commonly studied in environmental biotransformation by microorganisms or in human metabolism, but might contribute to the formation of currently still unknown TPs in the environment. The observed pathways are likely to have broader validity, e.g. pterin formation for sulfonamides in general; and glutamate conjugation for other fenamates, salicylates and benzoates.

Acknowledgements

We thank Dr. Marius Roos-Majewsky (Heidelberg University Hospital, Dept. of Clinical Pharmacology and Pharmacoepidemiology, Heidelberg, Germany) and Rafael Peschke (Karlsruher Institut für Technologie, Karlsruhe, Germany) for providing authentic standard of N4-hydroxyacetyl-sulfamethoxazole and helpful discussion. We thank Christian Ahrens (Agroscope, Wädenswil, Switzerland) and Cresten Mansfeldt (Eawag, Switzerland) for advice on bioinformatics. Dr. Emma Schymanski and Dr. Jennifer Schollée are acknowledged for helpful comments on the manuscript.

This work was supported by the Swiss National Science Foundation, grant number 315230_141190 and 205320_165935.

References

1 OECD, Environment Monograph No. 77. Data Requirements for Pesticide Registration in OECD Member Countries: Survey Results, 1994.
2 Committee for Medicinal Products for Human Use (CHMP), 2006.
3 OECD, OECD Guideline for the Testing of Chemicals: Aerobic and Anaerobic Transformation in Aquatic Sediment Systems, 2002.
4 OECD, OECD Guideline for the Testing of Chemicals: Aerobic Mineralisation in Surface Water - Simulation Biodegradation Test, 2004.
5 K. A. Thomas and L. H. Hand, Environ. Toxicol. Chem., 2011, **30**, 622–31.
6 K. A. Thomas and L. H. Hand, Environ. Toxicol. Chem., 2012, **31**, 2138–46.
7 Z. N. Norvill, A. Shilton and B. Guieysse, J. Hazard. Mater., 2016, **313**, 291–309.
8 I. de Godos, R. Muñoz and B. Guieysse, J. Hazard. Mater., 2012, **229**–**230**, 446–449.
9 A. de Wilt, A. Butkovskyi, K. Tuantet, L. Hernandez, T. V. Fernandes, A. Langenhoff and G. Zeeman, J. Hazard. Mater., 2016, 304, 84–92.
10 G.-J. Zhou, G.-G. Ying, S. Liu, L.-J. Zhou, Z.-F. Chen and F.-Q. Peng, Environ. Sci. Process. Impacts, 2014, **16**, 2018–2027.
11 A. Papazi and K. Kotzabasis, PLOS ONE, 2013, **8**, e61682.
12 G. H. LeFevre, C. E. Müller, R. J. Li, R. G. Luthy and E. S. Sattely, Environ. Sci. Technol., 2015, 49 (18), 10959–10968.
13 G. H. LeFevre, A. C. Portmann, C. E. Müller, E. S. Sattely and R. G. Luthy, Environ. Sci. Technol., 2016, **50**, 6762–6771.
14 D. W. Nebert, D. R. Nelson and R. Feyereisen, Xenobiotica, 1989, **19**, 1149–1160.
15 F. O. Robert, J. Pandhal and P. C. Wright, Curr. Opin. Microbiol., 2010, **13**, 301–306.
16 D. R. Nelson, Phytochem. Rev., 2006, **5**, 193–204.
17 S. Pflugmacher, C. Wiencke and H. Sandermann, Mar. Environ. Res., 1999, **48**, 23–36.
18 F. Thies and L. H. Grimme, Arch. Microbiol., 1995, **164**, 203–211.
19 M. Della Greca, G. Pinto, P. Pistillo, A. Pollio, L. Previtera and F. Temussi, Chemosphere, 2008, **70**, 2047–53.
20 K. Lai, M. Scrimshaw and J. Lester, Appl. Environ. Microbiol., 2002, **68**, 859–864.
21 F. Peng, G. Ying, B. Yang, S. Liu, H. Lai, Y. Liu, Z. Chen and G. Zhou, Chemosphere, 2014, **95**, 581–588.
22 H. M. Maes, S. X. Maletz, H. T. Ratte, J. Hollender and A. Schae, Environ. Sci. Technol., 2014, **48**, 12354–12361.
23 S. Rasoul-Amini, E. Fotooh-Abadi and Y. Ghasemi, J. Appl. Phycol., 2010, **23**, 975–981.
24 T. Cáceres, M. Megharaj and R. Naidu, Sci. Total Environ., 2008, **398**, 53–59.
25 F.-Q. Peng, G.-G. Ying, B. Yang, Y.-S. Liu, H.-J. Lai, G.-J. Zhou, J. Chen and J.-L. Zhao, Environ. Toxicol. Chem., 2014, **33**, 1705–1711.
26 X. Huang, Y. Tu, C. Song, T. Li, J. Lin, Y. Wu, J. Liu and C. Wu, Aquat. Toxicol., 2016, **172**, 103–110.
27 J. A. Zarn, B. J. Brüschweiler and J. R. Schlatter, Environ. Health Perspect., 2003, **111**, 255–261.
28 S. Huntscha, H. P. Singer, C. S. McArdell, C. E. Frank and J. Hollender, J. Chromatogr. A, 2012, **1268**, 74–83.
29 C. D. Broeckling, F. A. Afsar, S. Neumann, A. Ben-Hur and J. E. Prenni, Anal. Chem., 2014, **86**, 6812–7.
30 M. A. Stravs, E. L. Schymanski, H. P. Singer and J. Hollender, J. Mass Spectrom., 2013, **48**, 89–99.
31 H. Horai, M. Arita, S. Kanaya, Y. Nihei, T. Ikeda, K. Suwa, Y. Ojima, K. Tanaka, S. Tanaka, K. Aoshima, Y. Oda, Y. Kakazu, M. Kusano, T. Tohge, F. Matsuda, Y. Sawada, M. Y. Hirai, H. Nakanishi, K. Ikeda, N. Akimoto, T. Maoka, H. Takahashi, T. Ara, N. Sakurai, H. Suzuki, D. Shibata, S. Neumann, T. Iida, K. Tanaka, K. Funatsu, F. Matsuura, T. Soga, R. Taguchi, K. Saito and T. Nishioka, J. Mass Spectrom., 2010, **45**, 703–14.
32 M. Meringer, S. Reinker, J. Zhang and A. Muller, MATCH Commun. Math. Comput. Chem., 2011, **65**, 259–290.

33 F. Allen, R. Greiner and D. Wishart, Metabolomics, 2014, **11**, 98–110.
34 F. Allen, A. Pon, M. Wilson, R. Greiner and D. Wishart, Nucleic Acids Res., 2014, **42**, 94–99.
35 C. A. Smith, G. O'Maille, E. J. Want, C. Qin, S. A. Trauger, T. R. Brandon, D. E. Custodio, R. Abagyan and G. Siuzdak, Ther. Drug Monit., 2005, **27**, 747–51.
36 E. L. Schymanski, J. Jeon, R. Gulde, K. Fenner, M. Ruff, H. P. Singer and J. Hollender, Environ. Sci. Technol., 2014, **48**, 2097–2098.
37 M. A. Stravs, J. Mechelke, P. L. Ferguson, H. Singer and J. Hollender, Anal. Bioanal. Chem., 2016, **408**, 1879-1890.
38 T. R. Roberts and D. H. Hutson, in Metabolic Pathways of Agrochemicals: Part 2: Insecticides and Fungicides, eds. T. R. Roberts and D. H. Hutson, Royal Society of Chemistry, Cambridge, 1999, pp. 1327–1342.
39 J. A. Turner, The Pesticide Manual - A World Compendium, BCPC, Alton, 17th Editi., 2015.
40 J. Radjenović, S. Pérez, M. Petrović and D. Barceló, J. Chromatogr. A, 2008, **1210**, 142–153.
41 S. Kern, R. Baumgartner, D. E. Helbling, J. Hollender, H. Singer, M. J. Loos, R. P. Schwarzenbach and K. Fenner, J. Environ. Monit., 2010, **12**, 2100–11.
42 A. Rubirola, M. Llorca, S. Rodriguez-Mozaz, N. Casas, I. Rodriguez-Roda, D. Barceló and G. Buttiglieri, Water Res., 2014, **63**, 21–32.
43 J. McGourty, J. Silas, M. Lennard, G. Tucker and H. Woods, Br. J. Clin. Pharmacol., 1985, **20**, 555–566.
44 M. K. Richter, A. Focks, B. Siegfried, D. Rentsch, M. Krauss, R. P. Schwarzenbach and J. Hollender, Environ. Pollut., 2013, **172**, 208–15.
45 V. Prabhu, H. Lui and J. King, Phytochemistry, 1997, **45**, 23–27.
46 S. Roland, R. Ferone, R. J. Harvey, V. L. Styles and R. W. Morrison, J. Biol. Chem., 1979, **254**, 10337–45.
47 Y. L. Hong, P. A. Hossler, D. H. Calhoun and S. R. Meshnick, Antimicrob. Agents Chemother., 1995, **39**, 1756–1763.
48 E. A. Cossins, Botany, 2000, **78**, 691.
49 M. Majewsky, D. Wagner, M. Delay, S. Bräse, V. Yargeau and H. Horn, Chem. Res. Toxicol., 2014, **27**, 1821–1828.
50 M. Majewsky, T. Glauner and H. Horn, Anal. Bioanal. Chem., 2015, **407**, 5707-5717.
51 H. K. Kroemer, J.-C. Gautier, P. Beaune, C. Henderson, C. R. Wolf and M. Eichelbaum, Naunyn. Schmiedebergs Arch. Pharmacol.,1999, **348**, 332–337.
52 J. J. McNeil, G. W. Mihaly, A. Anderson, A. W. Marshall, R. A. Smallwood and W. J. Louis, Br. J. Clin. Pharmacol., 1981, **12**, 411–5.
53 H. Horng and L. Z. Benet, Drug Metab. Dispos., 2013, **41**, 1923–1933.
54 G. L. Lamoureux and D. G. Rusness, in Xenobiotic Conjugation Chemistry, American Chemical Society, 1986, **299**, 62–105.
55 P. E. Staswick, Plant Cell, 2002, **14**, 1405–1415.
56 P. E. Staswick, Plant Cell, 2005, **17**, 616–627.
57 V. M. Markowitz, I.-M. A. Chen, K. Chu, E. Szeto, K. Palaniappan, M. Pillay, A. Ratner, J. Huang, I. Pagani, S. Tringe, M. Huntemann, K. Billis, N. Varghese, K. Tennessen, K. Mavromatis, A. Pati, N. N. Ivanova and N. C. Kyrpides, Nucleic Acids Res., 2014, **42**, D568–D573.
58 V. M. Markowitz, I.-M. A. Chen, K. Palaniappan, K. Chu, E. Szeto, M. Pillay, A. Ratner, J. Huang, T. Woyke, M. Huntemann, I. Anderson, K. Billis, N. Varghese, K. Mavromatis, A. Pati, N. N. Ivanova and N. C. Kyrpides, Nucleic Acids Res., 2014, **42**, D560–D567.
59 R. A. Okrent, M. D. Brooks and M. C. Wildermuth, J. Biol. Chem., 2009, **284**, 9742–9754.
60 AstraZeneca, 2013, Environmental Risk Assessment Data: Atenolol, https://www.astrazeneca.com/content/dam/az/our-company/Sustainability/Atenolol.pdf
61 L. Sitoki, R. Kurmayer and E. Rott, Hydrobiologia, 2012, **691**, 109–122.
62 T. R. Roberts and D. H. Hutson, in *Metabolic Pathways of Agrochemicals : Part 2: Insecticides and Fungicides*, ed. T. R. Roberts and D. H. Hutson, Royal Society of Chemistry, Cambridge, 1999, pp. 1011-1104.

63 F. Thies and L. H. Grimme, Pestic. Sci., 1996, **47**, 337–346.
64 R. Gulde, U. Meier, E. L. Schymanski, H.-P. E. Kohler, D. E. Helbling, S. Derrer, D. Rentsch and K. Fenner, Environ. Sci. Technol., 2016, **50**, 2908–2920.
65 D. R. Johnson, D. E. Helbling, T. K. Lee, J. Park, K. Fenner, H. P. E. Kohler and M. Ackermann, Appl. Environ. Microbiol., 2015, **81**, 666–675.
66 K. Venkatakrishnan, L. L. von Moltke and D. J. Greenblatt, Clin. Pharmacokinet., 2000, **38**, 111–180.
67 B. Ferrari, R. Mons, B. Vollat, B. Fraysse, N. Paxēaus, R. L. Giudice, A. Pollio and J. Garric, Environ. Toxicol. Chem., 2004, **23**, 1344–1354.
68 M. O. Islam, M. Hara and J. Miyake, Environ. Toxicol. Pharmacol., 2002, **12**, 1–6.
69 N. Hanioka, H. Jinno, T. Nishimura and M. Ando, Chemosphere, 1997, **34**, 719–30.
70 D. R. Orvos, D. J. Versteeg, J. Inauen, M. Capdevielle, A. Rothenstein and V. Cunningham, Environ. Toxicol. Chem., 2002, **21**, 1338–1349.
71 A. Bérard, U. Dorigo, I. Mercier, K. Becker-van Slooten, D. Grandjean and C. Leboulanger, Chemosphere, 2003, **53**, 935–944.
72 J. A. Weiner, M. E. DeLorenzo and M. H. Fulton, Aquat. Toxicol., 2004, **68**, 121–128.
73 X. Deng, K. Gao and J. Sun, Aquat. Toxicol., 2012, **122**–**123**, 113–119.